Faujasite-Supported Ir_4 Clusters: A Density Functional Model Study of Metal−Zeolite Interactions

Anna Maria Ferrari,[†,‡] Konstantin M. Neyman,[†] Markus Mayer,[†] Markus Staufer,[†] Bruce C. Gates,[§,||] and Notker Rösch*[,†]

Lehrstuhl für Theoretische Chemie, Technische Universität München, D-85747 Garching, Germany, Dipartimento di Scienza dei Materiali, Istituto Nazionale della Materia, via Cozzi 53, I-20125 Milano, Italy, and Institut für Physikalische Chemie, Universität München, Butenandtstrasse 5-13 (Haus E), D-81377 München, Germany

Received: February 1, 1999; In Final Form: April 14, 1999

The interaction of a metal cluster, Ir_4, and a zeolite support was investigated computationally with the aid of a density functional method and a cluster model of a zeolite, i.e., a six-ring consisting of six O atoms and six T (Si or Al) atoms facing a supercage of a faujasite framework. Structural parameters are reported for an Ir_4 tetrahedron interacting with the zeolite six-ring. The calculations indicate two Ir−O distances, which match those reported on the basis of EXAFS spectroscopy at about 2.1−2.2 and 2.5−2.7 Å for various transition and noble metal clusters on zeolite (and metal oxide) supports, including Ir_4 in the supercages of zeolite NaY. The calculations indicate an Ir−Ir distance of about 2.5 Å, only a few hundredths of an Ångstrom more than the value calculated for the free Ir_4 cluster, but about 0.2 Å less than the values observed repeatedly by EXAFS spectroscopy for zeolite-supported clusters approximated as Ir_4. The experimental distances characterizing the zeolite-supported clusters are in close agreement with the crystallographic and calculated value reported for the coordinatively saturated cluster $Ir_4(CO)_{12}$ and favor the suggestion that the supported clusters investigated with EXAFS spectroscopy were not entirely ligand free (i.e., that their formation by decarbonylation of the parent $Ir_4(CO)_{12}$ did not proceed by simple, complete removal of CO ligands). Consequently, calculations were performed for unsupported model clusters Ir_4 with single H or C atoms as ligands; the results match the EXAFS data characterizing the Ir−Ir distance and favor the suggestion of carbon on the zeolite-supported clusters. The bonding of a single CO molecule to the supported Ir_4 at the on-top site was also modeled to probe changes in the electronic structure of the metal cluster in comparison with an unsupported metal cluster. The results show that the interaction of the metal cluster with the zeolite fragment induces a notable electron donation from the support to the metal cluster; it also causes a moderate charge rearrangement in the bonding region between the Ir and O centers, accompanied by a considerable polarization of the electron density toward the apex of the cluster not interacting directly with the zeolite. Generalizing this result, we suggest that small noble metal clusters interacting mainly with basic oxygen atoms of zeolite and metal oxide supports are nearly zerovalent or slightly negatively charged and that some effects of supports in catalysis may be explained by this charge transfer and by polarization.

Introduction

Metals are among the most important catalysts, usually being applied as small clusters or particles dispersed on the surfaces of metal oxide or zeolite supports.[1] The smaller the clusters or particles, the larger the fraction of the metal atoms exposed at a surface and accessible to reactants and available for catalysis. Zeolites are appealing supports, as they incorporate small, uniform pores that may stabilize small, nearly uniform metal clusters.[2−4] Much work has been devoted to the characterization of zeolite-supported metal clusters and particles.[3−15] Extended X-ray absorption fine structure (EXAFS) spectroscopy has indicated metal clusters as small as four atoms each in zeolites.[8,9,16−19] EXAFS spectroscopy is particularly successful for characterization of these materials because the supported clusters are so small that a large fraction of the metal is in contact with the support and a large part of the EXAFS signal is determined by metal−support contributions, providing information about the metal−support interface.

Because conventional preparation techniques result in nonuniform supported metal clusters and particles that are difficult to characterize well, attempts have been made to prepare nearly uniform supported metal clusters by synthesis of zeolite-supported molecular and ionic metal carbonyl cluster precursors and treatment to remove the carbonyl ligands with minimal disruption of the metal frame. However, the decarbonylation typically leads to fragmentation and/or aggregation of metal clusters, often with migration of the metal outside the zeolite pores,[2,15] and only a few supported metals with nearly uniform and rather well-defined structures have been prepared, e.g., Rh_6 in zeolite NaY[16] and Ir_4 and Ir_6 on metal oxides (MgO and γ-Al_2O_3) and zeolites (KLTL, NaX, and NaY).[16−25] Since iridium offers the advantage of giving clusters with quite stable metal frames (e.g., Ir_4 and Ir_6), such supported metal clusters have been most thoroughly investigated.[26]

* Corresponding author.
† Technische Universität München.
‡ Istituto Nazionale della Materia.
§ Universität München.
|| Permanent address: Department of Chemical Engineering and Materials Science, University of California, Davis, CA 95616.

10.1021/jp990369e CCC: $18.00
Published on Web 06/06/1999

Notwithstanding the substantial work on such samples, several questions remain, associated with the limitations of EXAFS spectroscopy as a characterization method and the lack of other incisive experimental techniques for investigation of such small entities dispersed in porous solids. Some of the questions are the following:

(i) What is the nature of the interaction between the metal clusters and the support?[25]

(ii) Why is the capacity for chemisorption of hydrogen or CO apparently less for these clusters than for supported particles of the same metal that are only slightly larger?[27]

(iii) Why is the catalytic activity of such clusters less than that of slightly larger supported particles of the same metal, even for structure-insensitive reactions?[28]

In attempts to shed light on these issues, and in particular to clarify how the interaction with a zeolite framework can modify the structural and electronic properties of small supported metal clusters, we have carried out a computational investigation of the interaction between small metal clusters and a zeolite fragment with the aid of a density functional (DF) approach using cluster models. The clusters were chosen to be Ir_4 because there is so much experimental information available for comparison. In this work we have gone beyond the earlier work of Jansen and van Santen,[29] in which the polarizing effect of a substrate was mimicked by a Mg^{2+} ion interacting with an Ir_4 cluster. We shall address the following specific questions:

(i) How are the structural parameters of supported Ir_4 clusters modified relative to those of free Ir_4 clusters and known molecular metal clusters exemplified by $Ir_4(CO)_{12}$?

(ii) How does the zeolite framework influence the electronic properties of supported Ir_4 clusters?

(iii) What changes in the electronic structure of the cluster that result from its interaction with the support can be deduced with the help of the C−O vibrational frequency of a CO probe molecule adsorbed on the supported cluster?

Computational Method and Models

The calculations were carried out at the DF level of theory with the help of a scalar-relativistic variant of the linear combination of Gaussian-type orbitals density functional method (LCGTO-DF)[30,31] as implemented in the new program ParaGauss for employing parallel computers.[32−34] Spin-polarized calculations were performed to account for the possible open-shell nature of the metal clusters. Large and flexible Gaussian-type basis sets were used to represent the Kohn−Sham orbitals. For Ir, a (19s,14p,10d,5f) basis set[35] was supplemented by two s (0.0117, 0.2222), three p (0.02938, 0.07345, 0.18363), two d (0.05639, 0.14097), and two f exponents (0.14391, 0.57564). The resulting basis set (21s,17p,12d,7f) was contracted to [10s,8p,5d,3f]. For C and O, basis sets of the type (9s,5p,2d) → [5s,4p,2d] were adopted.[36,37] Si and Al atoms were described by a (12s,9p,2d) → [6s,4p,2d] basis set[38] (with d exponents 1.1206, 0.3202 for Si and 1.0084, 0.2881 for Al).[39] A basis set of the type (12s,8p,2d) → [6s,5p,2d] (with d exponents 0.122 and 0.01825) was used for Na.[38,40] H atoms were described by the basis set (6s,2p) → [3s,2p].[36,37] All contractions were of generalized form based on atomic Kohn−Sham eigenvectors of local density calculations (of scalar-relativistic nature in the case of Ir). The auxiliary basis set employed in the LCGTO-DF method to represent the electron charge density was constructed by properly scaling the s and p exponents of the orbital basis sets in a standard fashion;[30] for Ir, only every second p-type exponent was used in constructing $d(r^2)$-type fitting functions. Furthermore, a set of five p- and five d-type polarization exponents located on each atom was added to the auxiliary basis set.[41] The fitted charge density was used to calculate the classic Coulomb contributions to the electron−electron interaction. The exchange-correlation energy and the matrix elements of the exchange-correlation potential were evaluated by numerical integration.[42,43]

The geometries of the various molecular systems were optimized by using analytical energy gradients.[44] Harmonic vibrational frequencies were derived from force constants calculated numerically with a finite difference approach. These calculations were carried out by employing the local spin density (LSD) approximation.[45]

The accuracy of the LSD functional for describing properties of adsorbed Ir_4 clusters was confirmed by calculations representing the parent compound $Ir_4(CO)_{12}$, which has been characterized in the solid state by X-ray diffraction crystallography[46] and by EXAFS spectroscopy.[47] Pertinent computed parameters are the bond distances $d(\mathrm{Ir-Ir}) = 2.694$ Å and $d(\mathrm{Ir-O}) = 3.030$ Å as well as the CO vibrational frequency shift $\Delta\omega(\mathrm{CO}) = -24$ cm^{-1} (with respect to the free CO molecule), in good agreement with the corresponding crystallographic values, $d(\mathrm{Ir-Ir}) = 2.693$ Å and $d(\mathrm{Ir-O}) = 3.009$ Å,[46] and the measured frequency shift $\Delta\omega(\mathrm{CO}) = -30$ cm^{-1},[48] and also in good agreement with the EXAFS bond distance, $d(\mathrm{Ir-Ir}) = 2.69$ Å.[47]

The tendency of the LSD approximation to overestimate binding energies is well established.[49] Nevertheless, binding energies evaluated with the help of the gradient-corrected (GC) BP functional (Becke's exchange functional[50] in combination with Perdew's correlation functional[51]) at the LSD geometry (denoted as BP//LSD) agree remarkably well with full BP//BP results (errors are only about 0.02 eV), as was demonstrated for CO adsorption on neutral and electronically modified Pt_4 clusters.[52] Thus, all binding energies in this work were calculated according to this economic and accurate BP//LSD procedure.[53] Binding energies are not corrected for the basis set superposition error since estimates for test systems based on the counterpoise method[54] indicate that such errors are only a small fraction of the computed binding energies (of the order of 0.1 eV).

The zeolite support was described by cluster models.[55] Zeolite NaY is one of the substrates (supports) used in experimental investigations of supported Ir_4 clusters;[17,26] these metal species are inferred to be located in the supercages (α-cages) of the zeolite. Therefore, to benefit from some symmetry constraints, it was decided to employ cluster models that represent the six-ring (a ring of six oxygen and six T centers, Si or Al) facing the supercage of the zeolite. The skeleton $Al_3Si_3O_6$ of this ring was derived from neutron and X-ray diffraction structure data.[56,57] The aluminum and silicon dangling bonds were saturated with hydrogen atoms,[55] and a C_3 symmetry constraint was imposed.

Two different models were constructed. In model A (Figure 1), $Al_3Si_3O_6H_{12}^{3-}$ (also referred to as Z), charge balancing by extraframework cations (which are present in the real zeolite framework) is ignored, and the cluster model is consequently charged. In model B, $Al_3Si_3O_6H_{12}Na_3$ (also denoted as Z-Na, Figure 1), three Na^+ ions were introduced in addition to build an electroneutral system that provides a more realistic model of a zeolite fragment. The Na^+ ions of Z-Na were located close to the oxygen centers O2 below the plane of the ring since the cations are associated with three six-rings adjacent to the ring under study and are therefore at the SI or SI′ positions in a faujasite framework.[56,57] Both models A and B were optimized by keeping the structure of the subunits $>SiH_2$ and $>AlH_2$ as well as their relative positions fixed. These constraints partially

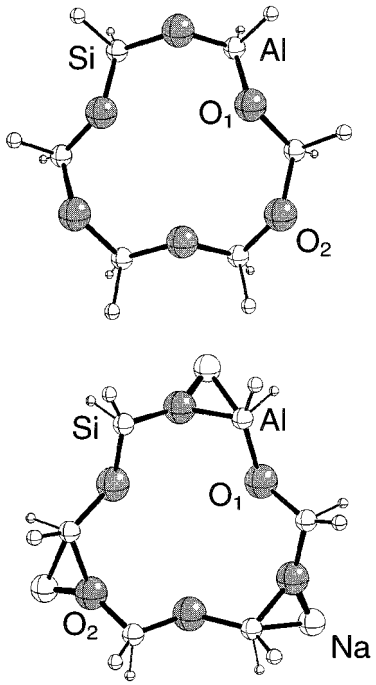

Figure 1. Cluster models used to describe a zeolite six-ring: Z−$Al_3Si_3O_6H_{12}^{3-}$ (top panel) and Z-Na−$Al_3Si_3O_6H_{12}Na_3$ (bottom panel).

TABLE 1: Computed Properties of the Cluster Models Z, $Al_3Si_3O_6H_{12}^{3-}$, and Z-Na, $Al_3Si_3O_6H_{12}Na_3$ (See Also Figure 1)[a]

	Z	Z-Na	exp[b]	exp[c]
d(Al−O_1)	1.709	1.729	1.65	1.72
d(Al−O_2)	1.753	1.785	1.65	1.72
d(Si−O_1)	1.584	1.599	1.65	1.62
d(Si−O_2)	1.608	1.650	1.65	1.62
d(O_1−O_1)	3.925	3.837	3.9	
d(O_2−O_2)	5.281	5.368	4.9	
d(O_2−Na)		2.140	2.24	2.22
∠(Al−O_1−Si)	146.3	142.6	146.2	145.5
∠(Al−O_2−Si)	141.1	134.6	146.2	134.8
q(O_1)	−0.61	−0.62		
q(O_2)	−0.64	−0.73		
BE(Na^+)[d]		23.21		
BE(Na^+)[e]		22.33		

[a] Distances d in Å, angles in degrees, Mulliken charges q in au, binding energy BE of Na^+ ions to Z in eV. [b] From ref 56. [c] From ref 57. [d] Computed at the LSD level. [e] Computed at the BP//LSD level.

resemble those of an actual zeolite framework; therefore, the model ring was not allowed to assume an arbitrary configuration. The resulting structures are very close to those determined experimentally. The results summarized in Table 1 show good agreement between pertinent computed and experimental structural parameters.

The cluster Ir_4 was adsorbed on both models Z and Z-Na, and three conceivable configurations were analyzed. In the first configuration (structure A, Figure 2), three metal centers at the base of the Ir_4 tetrahedron are located close to the oxygen centers O_1, whereas in the second configuration (structure B, Figure 2), the three base metal centers are placed closer to the centers O_2 of the model ring. Finally, the third structure (structure C, Figure 2) was derived from configuration A by reversing top and basal atoms of the Ir_4 cluster; i.e., the tip of the tetrahedron pointed into the six-ring. All structures were optimized by imposing a C_3 symmetry constraint; however, of the zeolite models, only the positions of the oxygen and sodium centers of the six-ring were allowed to relax.

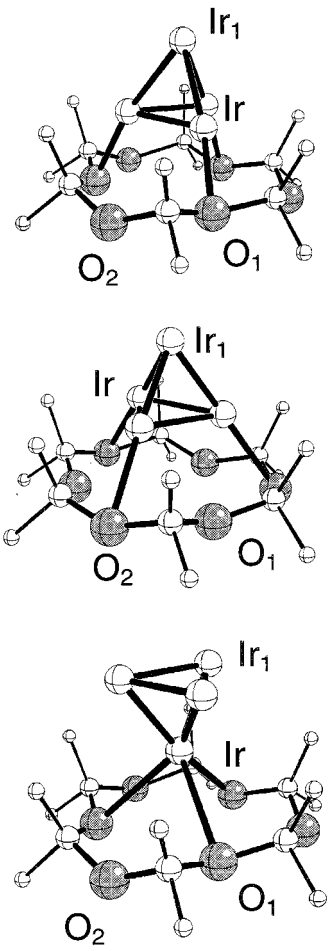

Figure 2. Ir_4 cluster supported on the zeolite fragment $Al_3Si_3O_6H_{12}^{3-}$: configuration A (top panel), configuration B (middle panel), and configuration C (bottom panel).

Results and Discussion

Properties of Supported Ir_4 and the Metal−Support Interface. Pertinent calculated results representing the adsorption properties of Ir_4 on the model rings Z and Z-Na are collected in Table 2. Analysis of second derivatives of the energy shows that the configurations A, B, and C of the supported Ir_4 (Figure 2) are local minima of the potential energy surface under the imposed constraints discussed in the previous section. The complex Ir_4(A)/Z is more stable than Ir_4(B)/Z by 1.92 (LSD) or 2.00 eV (BP//LSD). This stronger interaction also results in closer metal−support contacts, as exemplified by the distances between the metal atoms and the nearest oxygen centers; d(Ir−O_1) = 2.18 Å in Ir_4(A)/Z and d(Ir−O_2) = 2.66 Å in Ir_4(B)/Z. When the metal cluster interacts with the electrically neutral cluster model Z-Na, the resulting Ir_4(A)/Z-Na system is somewhat less stable than the complex Ir_4(A)/Z, by 0.67 (LSD) and 0.98 eV (BP//LSD), although no appreciable variations in the geometrical parameters can be observed between the two systems (Table 2). Structure C as described by the system Ir_4(C)/Z-Na is calculated to be slightly less stable than the corresponding configuration A, Ir_4(A)/Z-Na, by about 0.3 eV, concomitant with longer Ir−oxygen support distances; in Ir_4(A)/Z-Na and Ir_4(C)/Z-Na the shortest Ir−O distances d(Ir−O_1) are 2.24 and 2.33 Å, respectively (Figure 2 and Table 2).

The free Ir_4 cluster is characterized by a closed-shell electronic ground state $^1A_1$ (t_1^6); the effective electron configuration of the Ir atoms is $5d^{7.77}6s^{1.00}6p^{0.14}$, as derived from a

TABLE 2: Computed Properties of Complexes Ir_4/Z and Ir_4/Z-Na (See Also Figures 1 and 2)[a]

	Ir_4(A)/Z	Ir_4(A)/Z-Na	Ir_4(B)/Z	Ir_4(C)/Z-Na
d(Al−O_1)	1.725	1.747	1.727	1.802
d(Al−O_2)	1.776	1.803	1.717	1.821
d(Si−O_1)	1.611	1.632	1.599	1.656
d(Si−O_2)	1.617	1.660	1.598	1.669
d(O_1−O_1)	3.820	3.986	4.183	3.873
d(O_2−O_2)	5.361	5.492	5.272	5.593
∠(Al−O_1−Si)	141.9	137.8	142.8	131.4
∠(Al−O_2−Si)	138.1	132.4	145.9	130.4
d(Ir−O_1)	2.176	2.239	3.024	2.327
d(Ir−O_2)	3.488	3.486	2.660	3.301
d(Ir−Ir_1)[b]	2.450	2.442	2.432	2.451
d(Ir−Ir)[b]	2.479	2.499	2.533	
d(Ir_1−Ir_1)[b]				2.502
q(Ir)	−0.68	0.10	0.16	0.45
q(Ir_1)	−1.67	0.29	−0.42	−0.09
q(O_1)	−0.68	−0.70	−0.56	−0.69
q(O_2)	−0.64	−0.74	−0.59	−0.76
BE[c]	6.10	5.43	4.18	5.03
BE[d]	3.72	2.74	1.72	2.43
configuration	a^2e^4	a^2e^4	a^2e^4	a^2e^4
state	^1A	^1A	^1A	^1A

[a] Distances d in Å, angles in degrees, Mulliken charges q in au, binding energy BE of Ir_4 to Z and Z-Na in eV. [b] Free iridium clusters (T_d symmetry): Ir_4^+ t_1^5 ($^2T_1$), d(Ir−Ir)= 2.423 Å; Ir_4 t_1^6 ($^1A_1$), d(Ir−Ir) = 2.436 Å; Ir_4^- $t_1^6t_2^1$ ($^2T_2$), d(Ir−Ir) = 2.443 Å. [c] Computed at the LSD level. [d] Computed at the BP//LSD level.

Mulliken populations analysis. The triplet configuration $t_1^5t_2$ ($^3A_2$+^3E+$^3T_1$+$^3T_2$) lies 0.66 eV (BP//LSD) higher in energy; concomitantly, the ground state of Ir_4 exhibits a relatively large HOMO−LUMO gap, 0.63 eV, as measured by the Kohn−Sham eigenvalue difference. The closed-shell nature of the cluster Ir_4 is conserved upon adsorption, for all systems investigated (Table 2), as is the significant HOMO−LUMO gap (e.g., for the Ir_4(A)/Z-Na system, this gap is 0.58 eV).

As reported in Table 2, the shortest computed distances of Ir centers from support oxygen atoms are 2.18 (2.24) Å for Ir_4(A)/Z (Ir_4(A)/Z-Na) and 2.66 Å for Ir_4(B)/Z. It may be significant that these results correspond closely to the reported EXAFS parameters characterizing clusters of a number of metals (Ni, Rh, Pd, Re, Os, Ir, and Pt) on various metal oxide (SiO_2, γ-Al_2O_3, TiO_2, and MgO) and zeolite (LTL, X, and Y) supports; the EXAFS data indicate two metal−oxygen distances, one typically about 2.1−2.2 Å and the other about 2.5−2.7 Å.[58]

One explanation suggested for these distances is as follows. The longer metal−oxygen distance is normally observed by EXAFS spectroscopy when the metal is reduced in a H_2 atmosphere at a low temperature (<500 °C) whereas, after reduction at higher temperatures (> 600 °C), only a distance at about 2.2 Å was detected.[59,60] These results have been interpreted to suggest that the longer metal−support oxygen distance at 2.5−2.7 Å is observed when hydrogen is chemisorbed on the metal cluster and/or when the metal oxide surface is sufficiently hydroxylated. Therefore, it is possible that hydrogen is present at the interface between the metal species and the oxygen centers of the support, thereby increasing the metal−oxygen distance. This interfacial hydrogen is removed after treatment at high temperature, and consequently, only a short metal−support oxygen distance is observed.[58−60]

In this context, a comparison of the effect of substrate hydroxylation on the metal−support distances for Re(I) subcarbonyl adsorption at a corner-type cation vacancy of MgO seems useful. This system has been studied by EXAFS spectroscopy[61] and, very recently, by the same cluster model density functional approach used in the present work.[62] Both experiment and computation yielded a Re−O distance of 2.15 Å for the (almost fully) dehydroxylated MgO surface; on the other hand, the computational model of a hydroxyl covered surface resulted in a Re−O distance of 2.55 Å. Both distances agree very well with the two metal−oxygen ranges discussed above.

However, the distances referred to above have not always been observed, e.g., for Ir_4 clusters on MgO.[25] An alternative interpretation is that the longer metal−oxygen distances arise from weak interactions between the metal and the support, possibly when there is a geometric mismatch (a nonpseudomorphic fit) between the cluster and the support surface.[25] The calculated results seem to be in accord with this suggestion, although, in view of the simplified nature of our structural models, they are not sufficient to confirm it.

The shorter Ir−O distance approximately equals the sum of the covalent radii, r(Ir) = 1.27 Å and r(O) = 0.73 Å,[63] indicating a close approach of the metal moiety to the zeolite host. These values match metal−oxygen distances in metal complexes with oxygen-containing ligands, as determined by X-ray diffraction crystallography.[64,65] On the basis of the agreement of the metal−support oxygen distances of about 2.1 Å in supported metal clusters and the metal cation−oxygen distances, it was suggested that the metal−oxygen distance is a bonding distance and the supported clusters bear small positive charges.[64] The present results show that the metal−oxygen distance is not very sensitive to the charge on the zeolite fragment (cluster) used in the computations. Thus, we infer that the earlier suggestion[64] that metal oxide-supported clusters are positively charged is not borne out.

Ir−Ir Distances in Supported Ir_4 Clusters. In structures A and C, the longest Ir−Ir distance is calculated to be 2.50 Å, in Ir_4(A)/Z-Na and Ir_4(C)/Z-Na (Table 2). Thus, the computed Ir−Ir bond lengths are elongated by at most 0.06 Å with respect to the intermetal distance of the free Ir_4 cluster, d(Ir−Ir) = 2.436 Å.

The calculated contraction of the metal−metal bond length in free small metal particles relative to the bulk nearest-neighbor distance (Ir: 2.715 Å[66]) is not unexpected. A similar trend has been computed for small nickel, palladium, platinum, and gold clusters.[67−71] Metal clusters of 4−8 atoms exhibit nearest-neighbor distances that are contracted by about 10% relative to the corresponding bulk values; that distance increases gradually with the size of the cluster, converging to the bulk value.[67−69] Computed average nearest-neighbor distances scale essentially linearly with the average coordination number of the atoms in the clusters.[67−69]

Short internuclear distances in small metal clusters in general compensate for the effect of very low average coordination in these systems:[69,70] when the coordination numbers of metal atoms in small clusters are increased by the presence of ligands, the intermetal distance also elongates considerably.[72] A clear difference was found between low- and high-coordinated organometallic complexes.[69,70,72] In low-coordinated clusters, the computed metal−metal distances are considerably shorter (0.1−0.3 Å) than the bulk value, while the calculated intermetal distance is rather long and can even exceed the corresponding bulk value when the coordination shell is saturated.[70,72] A longer metal−metal distance than in the corresponding ligand-free metal cluster is also observed for $Ir_4(CO)_{12}$, investigated in the present work. The presence of 12 CO ligands, three for each Ir atom, results in an intermetal distance d(Ir−Ir) = 2.694 Å, very close to the Ir bulk value, 2.715 Å. The bare cluster Ir_4 is characterized by quite a strong cohesive energy, 3.23 eV per Ir atom

at the BP//LSD level. Nevertheless, the considerable binding energy between the 12 CO ligands and the iridium cluster, BE(BP//LSD) = 25.86 eV (2.15 eV per CO ligand and 6.45 eV per Ir atom), easily compensates the energetic cost necessary to expand the intermetal bonds of Ir_4 to their bulk length, 1.28 eV in total or 0.32 eV per Ir atom at the BP//LSD level.

When the Ir_4 moiety is bound to the zeolite fragment (Ir_4(A)/Z-Na, Table 2), the three iridium atoms at the base of the Ir_4 pyramid interact with the three closest framework oxygen centers. If we consider the zeolite oxygen centers as a multidentate ligand, by analogy to organometallic complexes, the bonding situation in the system Ir_4(A)/Z-Na reminds one of low-coordinated metal clusters since one counts one ligand each for the three metal centers at the base of the pyramidal cluster, whereas no ligand is bound to the atom at the top of the pyramid. Moreover, the computed binding energy of Ir_4 to the zeolite substrate, 0.85 eV per Ir atom (BP//LSD, Table 2), is much less than the corresponding value calculated for the complex $Ir_4(CO)_{12}$, 6.45 eV per Ir atom.

The situation in the system Ir_4(C)/Z-Na with its "inverted" geometry is similar (Figure 2). The binding energy of the Ir_4 moiety to the Z-Na fragment, BE = 2.43 eV (BP//LSD, Table 2), translates into 0.8 eV per Ir−O_1 interaction if one takes into account that the basal iridium center is bound to three oxygen centers of the zeolite substrate. This value is again considerably less than what is computed for the complex $Ir_4(CO)_{12}$, BE = 2.15 eV per Ir−CO bond.

On the basis of these considerations, it is not surprising that only a small elongation of the Ir−Ir distances is calculated for the model supported Ir_4. Notice that these arguments cannot be countered by claiming that the interaction between Ir_4 and the zeolite as described by the present cluster model is too weak. A somewhat larger binding energy (but one of similar magnitude), 1.24 eV per Ir atom (BP//LSD), is calculated for the charged model system (A)/Z (Table 2). The model Z yields the strongest possible interaction since the negative charge due to the presence of the three aluminum atoms is not compensated by extraframework cations as in the fragment Z-Na.

Finally, we also studied the charged moieties Ir_4^+ as a model of a cluster donating charge to the substrate and Ir_4^- as a model of an electron-enriched metal cluster. In this way, we estimated (the limits of) the effect of charge transfer on the structural parameters of the supported Ir_4 that seems possible in a zeolite cavity but may not be properly described by the present cluster models. Yet, even in these cases, no significant variation of the intermetal distances, at most ±0.01 Å, was computed (cf. footnote of Table 2). Thus, again, there is no reason to interpret the EXAFS metal−metal distances as a basis for inferring a charge on the metal cluster.

The computed intermetal bond distances of supported Ir_4 clusters are markedly different from the corresponding distances determined by EXAFS spectroscopy. EXAFS-determined Ir−Ir distances representing clusters approximated as Ir_4 supported on zeolites NaX and NaY and on γ-Al_2O_3 and MgO fall in the range 2.62−2.73 Å (with a typical value being 2.70 Å), very similar to the values for $Ir_4(CO)_{12}$, d(Ir−Ir) = 2.693 Å[46] and bulk Ir metal, d(Ir−Ir) = 2.715 Å.[66] A key question then is why is there a difference between the computed results and those observed by EXAFS spectroscopy? And why are all the metal−metal distances determined by EXAFS spectroscopy very close to the value for molecular metal complexes (such as metal carbonyls, illustrated by $Ir_4(CO)_{12}$), irrespective of the nature of the metal and of the support?[16,19,73−75] Several tentative explanations have been proposed, as follows.

One possibility is that a variety of structures of iridium clusters are present in the zeolite cages but not observed because of the experimental uncertainty in the EXAFS coordination numbers.[25] In this context, we recall that all our calculations were carried out under C_3 symmetry constraints. Of course, supported iridium clusters may exhibit distorted geometries, possibly even losing the pyramidal structure that has been assumed in the present work. However, the EXAFS first-shell coordination numbers are consistently near 3, the value for the Ir_4 tetrahedron, and we regard this possibility as unlikely.

We also note the suggestion that EXAFS estimates of metal−metal distances in metal particles may be in error because of vibrational anharmonicity effects which are not taken into account in the standard EXAFS analysis.[76] The inaccuracies were inferred to show up in high-temperature (300 K) data characterizing small copper particles, but not to be important at 100 K. As the EXAFS data discussed here were obtained at liquid-nitrogen temperature, we conclude that such errors are not significant in the present context. Furthermore, metal−metal distances in clusters approximated as Ir_4 in zeolite NaY were measured from liquid-nitrogen temperature up to room temperature, with no noticeable change in the Ir−Ir distance.[77] Furthermore, the accurate reproduction of the EXAFS result for the Ir−Ir distance in $Ir_4(CO)_{12}$[46,47] by our DF calculation indicates a lack of significant errors in the EXAFS-determined Ir−Ir distances. Thus, we regard it as unlikely that errors in the EXAFS analysis account for the discrepancy between the EXAFS data and the calculated results.

A more likely explanation is that the clusters in the zeolite cages carry ligands that are not detected by EXAFS because their atomic weights are low and EXAFS does not distinguish between low-Z backscatterers such as O and C. The possibility of carbon remaining from CO ligands has been suggested[27] for several reasons:

(i) The conversion of the precursor clusters $Ir_4(CO)_{12}$ in zeolite NaY proceeds by chemistry that is not yet well understood, and it is likely that it involves reaction of the CO ligands with the support surface with breaking of C−O bonds; the chemistry may be analogous to that occurring in Fischer−Tropsch catalysis[78] and could account for the formation of C on the metal clusters.

(ii) The equilibrium amount of chemisorbed hydrogen on decarbonylated Ir_4 clusters on γ-Al_2O_3 is markedly less than that on only slightly larger iridium clusters, formed by aggregation of the precursor clusters in a H_2 atmosphere, which could lead to removal of carbon.[79] The low chemisorption capacity has been suggested as indicative of partial coverage of the metal, e.g., by carbon, which would reduce the degree of coordinative unsaturatation of the clusters.[27]

(iii) Supported metal clusters such as Ir_4 on metal oxide and zeolite supports have catalytic activities for a structure-insensitive reaction, toluene hydrogenation, that are lower than those of only slightly larger clusters, prepared as described in the preceding paragraph; these observations have also led to the suggestion that the clusters were partially covered.[27]

To address this point in more detail, we investigated how the structure of a (free) Ir_4 cluster is perturbed by the presence of an H or C ligand. Different coordinations were investigated (Figure 3): at the center of the tetrahedral metal clusters (T_d symmetry), the 2-fold bridge site (C_s symmetry restriction), and a 3-fold hollow site (C_{3v} symmetry); for H, on-top coordination (C_{3v}) was also investigated. Pertinent calculated parameters are reported in Table 3. The results representing these rather simple models show that a single H or C ligand located at a 2-fold

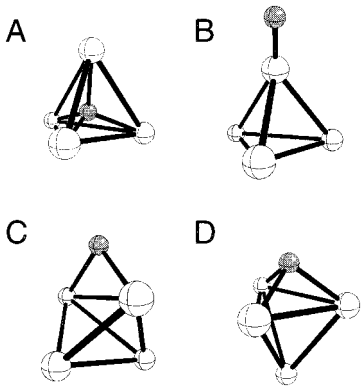

Figure 3. H or C ligand bound to a free Ir_4 cluster: (A) at the center of a tetrahedron (T_d symmetry); (B) at the on-top site (C_{3v} symmetry); (C) at the 2-fold bridge site (C_s symmetry); (D) at the 3-fold hollow site (C_{3v} symmetry). White spheres represent Ir atoms; gray spheres, H or C ligands.

bridge or C at a 3-fold hollow site of an Ir_4 cluster can account for a considerable elongation of the intermetal Ir−Ir distance. A carbon atom at a 2-fold bridge or 3-fold hollow site exhibits a substantial binding energy, BE = 7.9 and 7.5 eV, respectively (at the BP//LSD level, Table 3). This binding energy obtained for a free cluster likely represents an upper bound due to the unsaturated nature of the metal atoms. Invoking a bond-order conservation argument, we also expect a substantial chemisorption energy for a supported Ir_4 cluster interacting with a zeolite framework, in particular since the latter interaction is calculated to be moderate in comparison with that of a carbon atom. Note that an H defect at the center of a free Ir_4 cluster is less bound by about 2−3 eV than at the other positions considered, but even such a defect cluster may still exhibit some binding to the zeolite support. The present model calculations clearly demonstrate the possible significance of C (or H) ligands that could have formed during the reduction (decarbonylation) treatment and might not have been removed during the normal evacuation procedures.[25]

Properties of Adsorbed CO. An indirect but efficient way to monitor changes in the electronic structure of a supported metal cluster compared with a free metal moiety is to analyze the adsorption properties of a probe molecule. The most widely used probe molecule is CO because its vibrational stretching frequency ω(CO) is sensitive to small variations of the electronic structure at the adsorption site of a metal cluster or particle.[80] Many effects are involved in the interaction of a CO probe molecule with a metal substrate, including Pauli repulsion, σ donation, π back-donation, and substrate polarization.[81,82] However, analysis of the CO vibrational frequency shifts indicates that it is mainly related to the amount of back-donation from filled d orbitals of the metal particle to the empty antibonding $2\pi^*$ orbital of CO; Pauli repulsion from the metal substrate also plays a role.[82] Previously, we have studied the interaction of a CO probe molecule with neutral and charged Pt_4 clusters,[52] finding a linear relationship between the charge of the metal particle and the CO stretching frequency. We also showed that the vibrational frequency shift $\Delta\omega$(CO) can be correlated with the effective charge of the metal cluster (as induced by the presence of the substrate) when a Pt_4 cluster interacts with an electron-donating or -accepting support or with a ligand.

In the present investigation, we have analyzed the interaction properties of a CO probe molecule adsorbed at the on-top site of a supported Ir_4 cluster; adsorption complexes of both zeolite model clusters Z and Z-Na were investigated, CO−Ir_4(A)/Z and CO−Ir_4(A)/Z-Na (Table 4). Only the most stable complex, configuration A (Figure 2, Table 2), of the metal cluster bound to the zeolite subunit was considered. Moreover, to describe the computed vibrational shift $\Delta\omega$(CO) of the adsorbed probe molecule in terms of the effective charge of the supported Ir_4 cluster (as induced by the presence of the zeolite fragment), we elaborated the correlation between the C−O stretching frequency and the charge q of free clusters Ir_4^q. For this reason we studied the interaction of a CO molecule and neutral as well as charged Ir_4^q clusters, $q = +1, 0, -1$ au. Pertinent properties of these cluster models are collected in Table 4.

The shift $\Delta\omega$(CO) of the vibrational stretching frequency, with respect to the frequency of the free molecule, gradually moves to lower, more negative values when the electron count of the Ir_4 moiety increases, i.e., with the enhanced propensity for back-donation from the metal cluster to the CO ligand; see ref 52 for a detailed discussion. As for Pt_4, an almost linear correlation between $\Delta\omega$(CO) and the charge q of the Ir_4 moieties is found (Figure 4).

Now, we consider a CO probe molecule bound to an Ir_4 cluster supported on the neutral zeolite subunit, CO−Ir_4(A)/Z-Na. When CO is bound to the Ir_4(A)/Z-Na complex, its vibrational properties are quite different from those calculated for CO interacting with an unsupported Ir_4 cluster (Table 4). In particular, the vibrational shift $\Delta\omega$(CO), -192 cm^{-1}, of CO−Ir_4(A)/Z-Na is significantly larger in absolute value than that calculated for CO−Ir_4, -151 cm^{-1}. Consistent with this larger back-donation, we compute a slightly longer C−O bond distance in CO−Ir_4(A)/Z-Na, d(CO) = 1.161 Å, than in the unsupported cluster CO−Ir_4, d = 1.158 Å.

These findings clearly indicate that the interaction of the iridium cluster with the zeolite fragment Z-Na induces an electron density redistribution in the metal moiety. This conclusion is corroborated by an analysis of the electron density difference $\Delta\rho = \rho(Ir_4(A)/Z\text{-}Na) - \rho(Ir_4) - \rho(Z\text{-}Na)$ (Figure 5), which directly characterizes the charge rearrangement, avoiding possible pitfalls of a Mulliken analysis. Inspection of $\Delta\rho$ shows that the interaction between the cluster Ir_4 and the zeolite fragment Z-Na induces a moderate charge rearrangement in the bonding region between the centers Ir and O_1, accompanied by a considerable polarization of the electron density toward the "pyramid top" of the metal cluster (Figure 5). An alternative criterion for the effective charge on the Ir_4 cluster supported on the Z-Na zeolite fragment can be derived from the CO vibrational frequency shift via the linear relationship between ω(CO) and the charge q of the cluster Ir_4, as displayed in Figure 4. In this way, an effective charge value of $q = -0.45$ au is deduced from the calculated frequency shift value of $\Delta\omega$(CO) = -192 cm^{-1}. As a check, we also calculated the properties of CO adsorbed on a charged (free) model cluster $Ir_4^{-0.45}$ with a fractional charge matching the effective value derived from the CO vibrational frequency shift. Excellent agreement is found between calculated C−O and Ir−CO vibrational frequencies of the target complex CO−Ir_4(A)/Z-Na and the model CO−$Ir_4^{-0.45}$ (Table 4).

A somewhat different scenario emerges for CO adsorption on the charged cluster model Ir_4(A)/Z. In the complex CO−Ir_4(A)/Z, the CO bond distance is considerably elongated, d(CO) = 1.186 Å, in comparison with the corresponding value computed for the CO−Ir_4 complex, d(CO) = 1.158 Å. At the same time, the stretching frequency ω(CO) is remarkably shifted toward lower values, by -311 cm^{-1}, with respect to the free-CO reference system (Table 4); this red-shift is about twice as large as calculated for CO adsorbed at the unsupported Ir_4 cluster, $\Delta\omega$(CO) = -151 cm^{-1} (Table 4). The system Ir_4/Z

TABLE 3: Selected Properties of the Interaction between an H or a C Ligand and a Free Ir_4 Cluster[a]

	H[b]				C[b]		
	on-top	center	bridge	hollow	center	bridge	hollow
d(Ir−Ir)[c]	2.430	2.617	2.590	2.429	2.951	2.960	2.714
	2.452		2.419	2.447		2.470	2.397
			2.432			2.390	
d(Ir−H)	1.650	1.603	1.772	1.903			
d(Ir−C)					1.805	1.785	1.873
BE[d]	2.97	−0.20	3.27	2.66	4.96	9.19	8.61
BE[e]	2.70	−0.32	2.87	2.14	4.35	7.94	7.47

[a] Distances d in Å, binding energy BE of an H or C ligand to Ir_4 in eV. [b] The ligands were located at the center of the cluster (T_d symmetry), at 2-fold bridge (C_s) and 3-fold hollow sites (C_{3v}); in addition, H was located at the on-top site (C_{3v}). d(Ir−Ir) = 2.436 Å for the free Ir_4 cluster. See also Figure 3. [c] The first value refers to the metal−metal distance adjacent to the H or C ligand. [d] Computed at the LSD level. [e] Computed at the BP//LSD level.

TABLE 4: Selected Properties of CO Adsorbed On-Top at the Cluster Models Ir_4(A)/Z-Na and Ir_4(A)/Z, as Well as On-Top of Free Ir_4 Clusters[a]

	CO−Ir_4^+	CO−Ir_4	CO−Ir_4(A)/Z-Na	CO−$Ir_4^{-0.45}$	CO−Ir_4^-	CO−Ir_4(A)/Z
d(C−O)[b]	1.141	1.158	1.161	1.166	1.176	1.186
d(Ir_1−C)	1.946	1.881	1.902	1.860	1.844	1.858
d(Ir_1−Ir)[c]	2.467	2.456	2.500	2.466	2.474	2.532
d(Ir−Ir)[c]	2.393	2.423	2.465	2.424	2.427	2.442
d(Ir−O_1)			2.265			2.213
BE(CO)[d]	2.34	2.73	2.27	2.97	3.44	3.10
BE(CO)[e]	1.67	1.94	1.66	2.18	2.63	2.34
ω(Ir−CO)	415	477	418	520	544	492
ω(CO)	2102	2011	1970	1968	1928	1851
$\Delta\omega$(CO)[b]	−60	−151	−192	−194	−234	−311
configuration	e^4a	e^4a^2	e^4a^2	$e^4a^2e^{0.45}$	e^4a^2e	e^4a^2
state	^{2}A	^{1}A	^{1}A		^{2}E	^{1}A

[a] Distances d in Å, binding energy BE of CO to Ir_4 substrates in eV, Ir_4−CO vibrational stretching frequency ω(Ir−CO), C−O stretching frequency ω(CO), and its adsorption-induced shift $\Delta\omega$(CO) in cm^{-1}. [b] Free CO: d(CO) = 1.134 Å, ω(CO) = 2162 cm^{-1}. [c] Free iridium clusters (T_d symmetry): Ir_4 t_1^6 ($^1A_1$), d(Ir−Ir) = 2.436 Å; Ir_4^- $t_1^6t_2^1$ ($^2T_2$), d(Ir−Ir) = 2.443 Å; Ir_4^+ t_1^5 ($^2T_1$), d(Ir−Ir) = 2.423 Å; $Ir_4^{-0.45}$ $t_1^6t_2^{0.45}$, d(Ir−Ir) = 2.440 Å. [d] Computed at the LSD level. [e] Computed at the BP//LSD level.

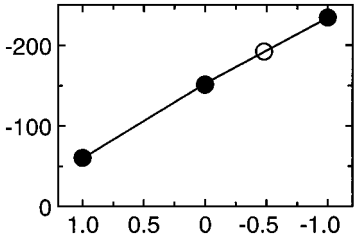

Figure 4. Dependence of the vibrational frequency shift $\Delta\omega$(CO) (in cm^{-1}) of the complexes CO−Ir_4 on the charge q (in au) of the cluster Ir_4^q (●) (see Table 4). Also shown is the frequency shift $\Delta\omega$(CO) (○) for CO adsorbed on the supported metal moiety Ir_4(A)/Z-Na. The CO probe molecule is adsorbed at the on-top position.

carries a negative charge because of the charged nature of the zeolite fragment Z, $Al_3Si_3O_6H_{12}^{3-}$. It is well-known[55] that the C−O bond distance elongates and the corresponding stretching frequency shifts to lower values when a CO probe molecule experiences an electric field. Nevertheless, the marked red-shift $\Delta\omega$(CO) computed for the system CO−Ir_4(A)/Z is not caused by the electric field created by the charged substrate moiety Z. In fact, a CO molecule vibrating at the same distance from a fragment Z as in the complex CO−Ir_4(A)/Z is characterized by a bond distance d(CO) = 1.138 Å and by a stretching frequency ω(C−O) = 2104 cm^{-1}, red-shifted by only 58 cm^{-1} with respect to the free CO molecule. Therefore, the considerable red-shift of the C−O stretching vibration, $\Delta\omega$(C−O) = −311 cm^{-1}, computed for CO−Ir_4(A)/Z must be associated with the propensity of the supported cluster Ir_4 to exhibit enhanced back-donation due to interaction with the negatively charged substrate Z, $Al_3Si_3O_6H_{12}^{3-}$. The effective charge of the metal cluster in the system Ir_4(A)/Z, as probed by the frequency shift $\Delta\omega$(CO),

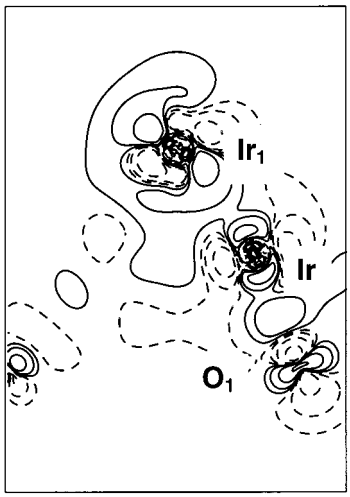

Figure 5. Electron density difference map $\Delta\rho = \rho(Ir_4(A)/Z\text{-Na}) - \rho(Ir_4) - \rho(Z\text{-Na})$. Solid and dashed lines indicate positive and negative values, respectively. The contours are drawn at $\pm 10^{-p}$ au, p = 2, 2.5, 3.

is quite large, about −2 au (Figure 4). However, this large charge redistribution onto the metal cluster is an *artifact* induced by the charged nature of the model cluster Z, $Al_3Si_3O_6H_{12}^{3-}$, employed to describe the zeolite substrate; it is not representative of the metal/support interaction that occurs in a zeolite cavity.

Implications Regarding Structures of Zeolite-Supported Metal Cluster Catalysts

An approach to understanding the nature of zeolite- and metal oxide-supported metal cluster catalysts involves synthesis of

small, nearly uniform supported clusters (e.g., Ir_4) from supported metal carbonyl precursors (e.g., $Ir_4(CO)_{12}$) and characterization by EXAFS spectroscopy, which is evidently the most incisive of the available experimental methods. We can now extend and improve the structural interpretations derived from the EXAFS data by invoking the theoretical results, as follows.

(i) The zeolite-supported Ir_4 clusters bear only a small negative charge, if any; we suggest that this statement may apply generally to noble metal clusters supported on metal oxides and zeolites. This suggestion is in line with the hypothesis of small, electron-rich Pt clusters formed in basic zeolites as a result of electron transfer from highly negatively charged framework oxygen atoms.[3] It has been proposed to rationalize X-ray photoelectron spectra, unusual catalytic properties, and a low intramolecular frequency of adsorbed CO. We have addressed the latter issue in a recent density functional study of Pt_4 species.[52] The present models of a six-ring (with a high Al-to-Si ratio of unity and the absence of charge-compensating bridging OH groups) are expected to mimic basic zeolites such as NaX.[3] We recognize that the presence of adsorbates (e.g., reactants) can influence the charge on the metal cluster and that the issues are complex.

(ii) Zeolite-supported Ir_4 clusters are characterized by a moderate charge rearrangement in the bonding region between the Ir and O centers, accompanied by polarization of the electron density toward the top side of the cluster. Such polarization effects might be responsible for some of the support effects observed in catalysis by supported metal clusters, and this point is worthy of further theoretical investigation.

(iii) The metal−metal distances observed by EXAFS spectroscopy indicate metal clusters that are probably not ligand-free, even after decarbonylation and evacuation under mild conditions; the EXAFS data are not sufficiently sensitive to give evidence of small numbers of ligands present in addition to the oxygen of the support, and theory evidently provides the best available method for establishing their likely presence.

(iv) Experimental work is recommended to search for and identify ligands on supported metal clusters prepared from metal carbonyl precursors following decarbonylation treatments. The experiments are expected to be challenging (a) because loadings of metal on the supports evidently need to be low (roughly 1 wt %) to facilitate high-yield synthesis of the supported metal carbonyl precursors, making quantitative experiments such as temperature-programmed decomposition challenging, and (b) because treatments under only moderately severe conditions to remove possible ligands (such as carbon that has been calculated to bind strongly to Ir_4) readily cause restructuring of the metal clusters (e.g., aggregation).[79]

Thus, the present results demonstrate how theory, used in concert with experiment, is helping to define opportunities for progress in research with supported metal catalysts. In the future, we anticipate that more powerful theoretical tools than those employed here will help to define the reaction intermediates on supported metal catalysts such as that investigated here. Because the reaction intermediates are usually highly reactive, they seem to be beyond the reach of current experimental methods such as in-situ EXAFS spectroscopy, which is likely to give evidence only of stable species and not reactive intermediates.

Conclusions

We have investigated theoretically the interaction between an Ir_4 cluster and a cluster model for a six-ring of a faujasite framework. Two models were used to describe the zeolite ring: a charged model Z, $Al_3Si_3O_6H_{12}^{3-}$, and a neutral model Z-Na, $Al_3Si_3O_6H_{12}Na_3$, where the negative charge induced by the presence of the three aluminum centers is compensated by three Na^+ ions, just as in alkali-exchanged zeolites. Considering structure and energetics, the two models yield a similar description of the main features of the metal−support interaction. The resulting most stable structures, Ir_4(A)/Z and Ir_4(A)/Z-Na (Figure 2), are characterized by quite strong binding energies, BE(BP//LSD) = 3.72 and 2.74 eV, respectively. The shortest metal−oxygen distance $d(Ir-O_1)$ is computed to be about 2.2 Å. This value, in good agreement with reported structural determinations by EXAFS spectroscopy, indicates a close approach of the metal to the zeolite fragment. The computed Ir−Ir intermetal distances are slightly elongated, up to 0.06 Å, in comparison with the value $d(Ir-Ir) = 2.436$ Å calculated for the free metal cluster. This result is at variance with EXAFS observations which indicate an intermetal distance, $d(Ir-Ir) \cong 2.7$ Å, very close to the corresponding value for crystalline $Ir_4(CO)_{12}$ (2.69 Å) and the metal bulk value, 2.715 Å. Possible reasons for this discrepancy have been analyzed. In particular, we show that the presence of an extra C ligand, residual from the reduction (decarbonylation) treatment, located at the 2-fold bridge or 3-fold hollow site of the Ir_4 cluster, can account for a considerable elongation in the Ir−Ir intermetal distance (Table 3). The unusually large discrepancy between calculated Ir−Ir distances and values derived from EXAFS measurements, about 0.2 Å, suggests that a further investigation of possible undetected ligands in zeolite-supported clusters may be worthwhile. This difference falls far outside the usual accuracy of density functional calculations, in particular for metal−metal distances.[67−69]

A CO molecule was chemisorbed at the on-top site of the metal cluster to probe the changes in the electronic structure of the metal particles induced by the zeolite support. When the zeolite substrate is described by the realistic Z-Na model, the interaction is accompanied by a small electron donation to the cluster, notable through a somewhat enhanced red-shift of the C−O stretching frequency. On the other hand, when the zeolite support is described by the charged cluster model Z, $Al_3Si_3O_6H_{12}^{3-}$, a substantial transfer of electron density from the zeolite fragment to the metal cluster was determined, in this case artificially induced by the charged nature of the zeolite cluster model.

Acknowledgment. We gratefully acknowledge stimulating discussions with J. K. Nørskov and G. Pacchioni. This work was supported by the Deutsche Forschungsgemeinschaft and the Fonds der Chemischen Industrie. B.C.G. thanks the Alexander von Humboldt Foundation and the U. S. Department of Energy, Office of Energy Research, Office of Basic Energy Sciences, Division of Chemical Sciences, contract FG02-87ER13790.

References and Notes

(1) Gates, B. C. *Catalytic Chemistry*; Wiley: New York, 1992.
(2) Sachtler, W. M. H.; Zhang, Z. *Adv. Catal*. **1993**, *39*, 129.
(3) Barthomeuf, D. *Catal. Rev*. **1996**, *38*, 521.
(4) Sachtler, W. M. H. *Acc. Chem. Res*. **1993**, *26*, 386.
(5) Stakheev, A. Y.; Shpiro, E. S.; Tkachenko, O. P.; Jaeger, N. I.; Schulz-Ekloff, G. *J. Catal*. **1997**, *169*, 382.
(6) McCarthy, T. J.; Marques, C. M. P.; Treviño, H.; Sachtler, W. M. H. *Catal. Lett*. **1997**, *43*, 11.
(7) Stakheev, A. Y.; Shpiro, E. S.; Jaeger, N. I.; Schulz-Ekloff, G. *Catal. Lett*. **1995**, *32*, 147.
(8) Khodakov, A.; Barbouth, N.; Oudar, J.; Villain, F.; Bazin, D.; Dexpert, H.; Schulz, P. *J. Phys. Chem*. **1997**, *101*, 766.

(9) Vaarkamp, M.; Modica, F. S.; Miller, J. T.; Koningsberger, D. C. *J. Catal*. **1993**, *144*, 611.
(10) Han, W.-J.; Kooh, A. B.; Hicks, R. F. *Catal. Lett*. **1993**, *18*, 193.
(11) Kappers, M. J.; Van der Maas, J. H. *Catal. Lett.* **1991**, *10*, 365.
(12) Kazansky, V. B.; Borovkov, V. Y.; Sokolova, M.; Jaeger, N. I.; Schulz-Ekloff, G. *Catal. Lett.* **1994**, *23***,** 263.
(13) Kustov, L. M.; Ostgard, D.; Sachtler, W. M. H. *Catal. Lett.* **1991**, *9*, 121.
(14) Besoukhanova, C.; Guidot, J.; Barthomeuf, D.; Breysse, M.; Bernard, J. R. *J. Chem. Soc., Faraday Trans. 1* **1981**, *77*, 1595
(15) Kawi, S.; Gates, B. C. In *Clusters and Colloids−From Theory to Applications*; Schmid, G., Ed.; Weinheim: VCH, 1994; p 299.
(16) Weber, W. A.; Gates, B. C. *J. Phys. Chem*. **1997**, *101*, 10423
(17) Kawi, S.; Chang, J. R.; Gates, B. C. *J. Phys. Chem*. **1993**, *97*, 10599.
(18) Kawi, S.; Gates, B. C. *J. Phys. Chem*. **1995**, *99*, 8824.
(19) Deutsch, S. E.; Miller, J. T.; Tomishige, K.; Iwasawa, Y.; Weber, W. A.; Gates, B. C. *J. Phys. Chem*. **1996**, *100*, 13408.
(20) Kawi, S.; Chang, J. R.; Gates, B. C. *J. Phys. Chem*. **1993**, *97*, 5375.
(21) Alexeev, O.; Panjabi, G.; Gates, B. C. *J. Catal.* **1998**, *173*, 196.
(22) Kawi, S.; Chang, J. R.; Gates, B. C. *J. Am. Chem. Soc*. **1993**, *115*, 4830.
(23) Maloney, S. D.; Kelley, M. J.; Koningsberger, D. C.; Gates, B. C. *J. Phys. Chem*. **1991**, *95*, 9406.
(24) Zhao, A.; Jentoft, R. E.; Gates, B. C. *J. Catal*. **1997**, *169*, 263.
(25) Deutsch, S. E.; Mestl, G.; Knözinger, H.; Gates, B. C. *J. Phys. Chem*. **1997**, *101*, 1374.
(26) Gates, B. C. In *Catalysis by Di- and Polynuclear Metal Cluster Complexes*; Adams, R. D., Cotton, F. A., Eds.; Weinheim: VCH, 1998; p 509.
(27) Alexeev, O.; Gates, B. C. *J. Catal*. **1998**, *176*, 310.
(28) Xu, Z.; Xiao, F.-S.; Purnell, S. K.; Alexeev, O.; Kawi, S.; Deutsch, S. E.; Gates, B. C. *Nature (London)* **1994**, *372*, 346.
(29) Jansen, A. P. J.; van Santen, R. A. *J. Phys. Chem.* **1990**, *94*, 6764.
(30) Dunlap, B. I.; Rösch, N. *Adv. Quantum Chem*. **1990**, *21*, 317.
(31) Rösch, N.; Krüger, S.; Mayer, M.; Nasluzov, V. A. In *Recent Development and Applications of Modern Density Functional Theory*. *Theoretical and Computational Chemistry*, Vol. 4; Seminario, J. M., Ed.; Elsevier: Amsterdam, 1996; p 497.
(32) Belling, T.; Grauschopf, T.; Krüger, S.; Nörtemann, F.; Staufer, M.; Mayer, M.; Nasluzov, V. A.; Birkenheuer, U.; Rösch, N. *ParaGauss 1.9*; Technische Universität München, 1998.
(33) Rösch, N.; Krüger, S.; Belling, T.; Nörtemann, F.; Staufer, M.; Zenger, C.; Grauschopf, T. In *HPSC97−Stand und Perspektiven des Parallelen Höchstleistungsrechnens*; Proceedings of the Statustagung des BMBF, February 1997, Munich, Germany; Wolf, H., Krahl, R., Eds.; Deutsche Forschungsanstalt für Luft- und Raumfahrt: Berlin, 1997; p 165.
(34) Belling, T.; Grauschopf, T.; Krüger, S.; Mayer, M.; Nörtemann, F.; Staufer, M.; Zenger, C.; Rösch, N. In *High Performance Scientific and Engineering Computing*; Proceedings of the First International FORTWIHR Conference, Munich, Germany, February 1998; Bungartz, H.-J., Durst, F., Zenger Chr., Eds.; Lecture Notes in Computational Science and Engineering; Springer: Heidelberg, 1999; p 439.
(35) Gropen, O. *J. Comput. Chem.* **1987,** *8*, 982.
(36) Van Duijneveldt, F. B. *IBM Res. Rep.* No. RJ 945, **1971**.
(37) Neyman, K. M.; Strodel, P.; Ruzankin, S. P.; Schlensog, N.; Knözinger, H.; Rösch, N. *Catal. Lett.* **1995**, *31*, 273.
(38) Veillard, A. *Theor. Chim. Acta* **1968**, *12*, 405.
(39) Strodel, P.; Neyman K. M.; Knözinger, H.; Rösch, N. *Chem. Phys. Lett.* **1995**, *240*, 542.
(40) Heiz, U.; Vayloyan, A.; Schumacher, E.; Yeretzian, C.; Stener, M.; Gisdakis, P.; Rösch, N. *J. Chem. Phys.* **1996**, *105*, 5574.
(41) Chung, S. C.; Krüger, S.; Pacchioni, G.; Rösch, N. *J. Chem. Phys*. **1995**, *102*, 3695.
(42) Pople, J. A.; Gill, P. M. W.; Johnson, B. G. *Chem. Phys. Lett*. **1992**, *199*, 557.
(43) Gill, P. M. W.; Johnson, B. G.; Pople, J. A. *Chem. Phys. Lett*. **1993**, *209*, 506.
(44) Nasluzov, V. A.; Rösch, N. *Chem. Phys.* **1996**, *210*, 413.
(45) Vosko, S. H.; Wilk, L.; Nusair, M. *Can. J. Phys.* **1980**, *58*, 1200.
(46) Churchill, M. R.; Hutchinson, J. P. *Inorg. Chem*. **1978**, *17*, 3529.
(47) Maloney, S. D. Ph.D. Dissertation, University of Delaware, Newark, DE, 1990.
(48) Psaro, R.; Dossi, C.; Fusi, A.; Della Pergola, R.; Garlaschelli, L.; Roberto, D.; Sordelli, L.; Ugo, R. *J. Chem. Soc., Faraday Trans*. **1992**, *88*, 369.
(49) *Recent Development and Applications of Modern Density Functional Theory*; Seminario, J. M., Ed.; Theoretical and Computational Chemistry, Vol. 4; Elsevier: Amsterdam, 1996.
(50) Becke, A. D. *Phys. Rev. A* **1988**, *38*, 3098.
(51) Perdew, J. P. *Phys. Rev. B* **1986**, *33*, 8622; **1986**, *34*, 7406.
(52) Ferrari, A. M.; Neyman, K. M.; Belling, T.; Mayer, M.; Rösch, N. *J. Phys. Chem. B* **1999**, *103*, 216.
(53) Fan, L.; Ziegler, T. *J. Chem. Phys*. **1991**, *95*, 7401.
(54) Boys, S. F.; Bernardi, F. *Mol. Phys.* **1970**, *19*, 553.
(55) Sauer, J.; Ugliengo, P.; Garrone, E.; Saunders, V. R. *Chem. Rev.* **1994**, *94*, 2095.
(56) Fitch, A. N.; Jobic, H.; Renouprez, A. *J. Phys. Chem.* **1986**, *90*, 1311.
(57) Olson, D. H. *Zeolites* **1995**, *15*, 439.
(58) Koningsberger, D. C.; Gates, B. C. *Catal. Lett.* **1992**, *14*, 271 and references therein.
(59) Vaarkamp, M.; Modica, F. S.; Miller, J. T.; Koningsberger, D. C. *J. Catal*. **1993**, *144*, 611.
(60) Miller, J. T.; Meyers, B. L.; Modica, F. S.; Lane, G. S.; Vaarkamp, M.; Koningsberger D. C. *J. Catal.* **1993**, *143*, 395.
(61) Kirlin, P. S.; van Zon, F. B. M.; Koningsberger, D. C.; Gates, B. C. *J. Phys. Chem.* **1990**, *94*, 8439.
(62) Hu, A.; Neyman, K. M.; Staufer, M.; Belling, T.; Gates, B. C.; Rösch, N. *J. Am. Chem. Soc*., in press.
(63) *Periodensystem der Elemente*; VCH Verlag: Weinheim, 1995.
(64) Chang, J.-R.; Gron, L. U.; Honji, A.; Sanchez, K. M.; Gates, B. C. *J. Phys. Chem*. **1991**, *95*, 9944.
(65) Gates, B. C.; Lamb, H. H. *J. Mol. Catal*. **1989**, *52*, 1.
(66) Wyckoff, R. W. G. *Crystal Structures*, 2nd ed.; Interscience Publishers: New York, 1965; Vol 1.
(67) Häberlen, O. D.; Chung, S. C.; Stener, M.; Rösch, N. *J. Chem. Phys*. **1997**, *106*, 5189.
(68) Krüger, S.; Vent, S.; Rösch, N. *Ber. Bunsen-Ges. Phys. Chem*. **1997**, *101*, 1640.
(69) Rösch, N.; Ackermann, L.; Pacchioni, G. *Chem. Phys. Lett*. **1992**, *199*, 275.
(70) Rösch, N.; Pacchioni, G. In *Clusters and Colloids − From Theory to Applications*; Schmid, G., Ed.; Weinheim: VCH, 1994; p 5.
(71) Dai, D.; Balasubramanian, K. *J. Chem. Phys*. **1995**, *103*, 648.
(72) Rösch, N.; Ackermann, L.; Pacchioni, G. *Inorg. Chem.* **1993**, *32*, 2963.
(73) Van Blik, H. F. J.; van Zon, J. B. A. D.; Huzinaga, T.; Vis, J. C.; Koningsberger, D. C. *J. Am. Chem. Soc*. **1985**, *107*, 3139.
(74) Samant, M. G.; Boudart, M. *J. Phys. Chem.* **1991**, *95*, 4070.
(75) Chang, J. R.; Koningsberger, D. C.; Gates, B. C. *J. Am. Chem. Soc.* **1992**, *114*, 6461.
(76) Hansen, L. B.; Stoltze, P.; Nørskov, J. K.; Clausen, B. S.; Niemann, W. *Phys. Rev. Lett.* **1990**, *64*, 3155.
(77) Weber, W. A.; Zhao, A.; Gates, B. C. *J. Catal*., in press.
(78) Smith, A. K.; Theolier, A.; Basset, J.-M.; Ugo, R.; Commereuc, D.; Chauvin, Y. *J. Am. Chem. Soc*. **1978**, *100*, 2590.
(79) Xiao, F.-S.; Weber, W. A.; Alexeev, O.; Gates, B. C. Proc. 11th Intl. Congr. Catal. (Baltimore); Elsevier: Amsterdam, 1996; Part B, p 1135.
(80) Marchese, L.; Boccuzzi, M. R.; Coluccia, S.; Lavagnino, S.; Zecchina, A.; Bonneviot, L.; Che, M. In *Structure and Reactivity of Surfaces*; Morterra, C., Zecchina, A., Costa, G., Eds.; *Studies in Surface Science and Catalysis*, Vol. 48; Elsevier: Amsterdam, 1989; p 653.
(81) Pacchioni, G.; Bagus, P. S. *J. Chem. Phys*. **1990**, *93*, 1209.
(82) Illas, F.; Zurita, S.; Márquez, A. M.; Rubio, J. *Surf. Sci.* **1997**, *376*, 279.